Protein Science (1994), *3*:898-910. Cambridge University Press. Printed in the USA.

Kringle–kringle interactions in multimer kringle structures

K. PADMANABHAN, T.-P. WU, K.G. RAVICHANDRAN,[1] AND A. TULINSKY
Department of Chemistry, Michigan State University, East Lansing, Michigan 48824

(RECEIVED February 15, 1994; ACCEPTED March 31, 1994)

Abstract

The crystal structure of a monoclinic form of human plasminogen kringle 4 (PGK4) has been solved by molecular replacement using the orthorhombic structure as a model and it has been refined by restrained least-squares methods to an *R* factor of 16.4% at 2.25 Å resolution. The X-PLOR structure of kringle 2 of tissue plasminogen activator (t-PAK2) has been refined further using PROFFT ($R = 14.5\%$ at 2.38 Å resolution). The PGK4 structure has 2 and t-PAK2 has 3 independent molecules in the asymmetric unit. There are 5 different noncrystallographic symmetry "dimers" in PGK4. Three make extensive kringle–kringle interactions related by noncrystallographic 2_1 screw axes without blocking the lysine binding site. Such associations may occur in multikringle structures such as prothrombin, hepatocyte growth factor, plasminogen (PG), and apolipoprotein [a]. The t-PAK2 structure also has noncrystallographic screw symmetry (3_1) and mimics fibrin binding mode by having lysine of one molecule interacting electrostatically with the lysine binding site of another kringle. This ligand-like binding interaction may be important in kringle–kringle interactions involving non-lysine binding kringles with lysine or pseudo-lysine binding sites. Electrostatic intermolecular interactions involving the lysine binding site are also found in the crystal structures of PGK1 and orthorhombic PGK4. Anions associate with the cationic centers of these and t-PAK2 that appear to be more than occasional components of lysine binding site regions.

Keywords: crystal packing interactions; kringle–kringle interactions; lysine binding site interactions; 2 and 3 molecules per asymmetric unit

Kringles are independent structural and functional folding domains that are 3-disulfide, triple-loop structures consisting of about 80 residues and are found in the noncatalytic regions of regulatory proteases of blood coagulation and fibrinolysis (Sottrup-Jensen et al., 1978; Patthy, 1985). It has been shown that kringles occur singly in UK-type PG activator (Gunzler et al., 1982; Steffens et al., 1982), factor XII (McMullen & Fujikawa, 1985), and vampire bat salivary PG activator (Gardell et al., 1989), as pairs in PT (Magnusson et al., 1975) and t-PA (Pennica et al., 1983), as 4 copies in hepatocyte growth factor (Nakamura et al., 1989), and as 5 in PG (Sottrup-Jensen et al., 1978). Most striking, however, is apolipoprotein [a], with 38 kringles, 37 of which are highly homologous to PGK4 (Fig. 1) and 1 of which resembles PGK5 (McLean et al., 1987). Kringles are usually accompanied by other noncatalytic folding domains such as the Ca^{+2} ion-mediated membrane binding Gla-domain (Gitel et al., 1973; Nelsestuen et al., 1974; Stenflo et al., 1974) and the epidermal growth factor-like module (Patthy, 1985). The latter can also occur as multiple copies.

Some kringles display protein recognition by interacting with macromolecules, thereby assisting enzyme specificity in biological processes. Thus, PTK2 associates with thrombin with a K_d in the nanomolar range (Myrmel et al., 1976; Arni et al., 1993) and can bind to the heavy chain of membrane bound factor Va in the prothrombinase complex (Esmon & Jackson, 1974) while PGK1, PGK4, and t-PAK2 bind fibrin, lysine, or, in general, ω-aminocarboxylic acids and ACA in particular (Hochschwender & Laursen, 1981; Trexler et al., 1982). The lysine binding site has been shown by modeling (Tulinsky et al., 1988a) and crystallography (Mulichak et al., 1991; Wu et al., 1991, 1994) to consist of doubly charged anionic and cationic centers in PGK1 and PGK4, although site-specific mutagenesis indicates that in solution only a monocationic center is operative in both (Hoover et al., 1993; Nielsen et al., 1993), while there is only a single positive charge in the cationic subsite of t-PAK2 (De Serrano et al., 1992; de Vos et al., 1992).

The PGK123 fragment and miniplasminogen (PGK5 with catalytic domain) also bind fibrin (Thorsen et al., 1981). The fibrin binding of both and of PGK4 is diminished by ACA, with the

Reprint requests to: Alexander Tulinsky, Department of Chemistry, Michigan State University, East Lansing, Michigan 48824; e-mail: tulinsky@cemvax.cem.msu.edu or tulinsky@msucem.bitnet.

Abbreviations: UK, urokinase; PG, plasminogen; PT, prothrombin; t-PA, tissue type plasminogen activator; PGK4, fourth kringle of PG; Gla, γ-carboxyglutamic acid; ACA, ε-aminocaproic acid; PGK123, kringles 1, 2, and 3 of PG; PTF1, PT1-156; PPACK, d-FPR chloromethylketone, where d- is d-enantiomer.

[1] Present address: Howard Hughes Medical Institute, University of Texas, Southwestern Medical Center at Dallas, 5323 Harry Hines Boulevard, Dallas, Texas 75235-9050.

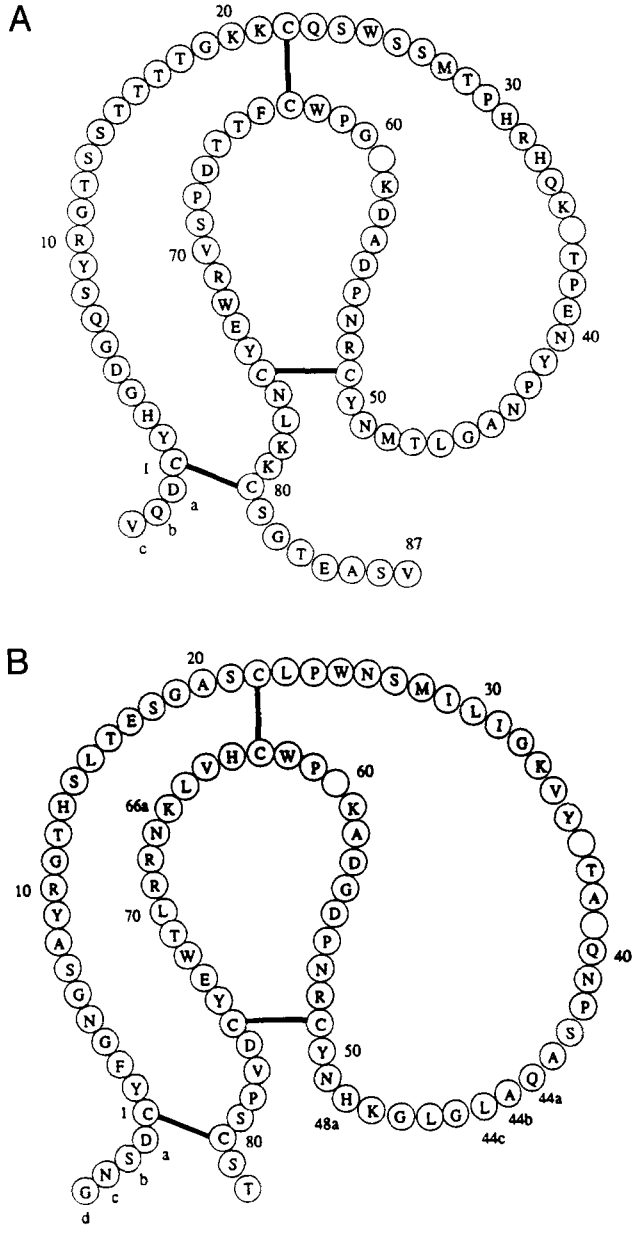

Fig. 1. Sequences of (**A**) PGK4 and (**B**) t-PAK2. Interkringle residues: a–c and 81–87 in PGK4, a–d in t-PAK2; 81–82 links to catalytic domain of t-PAK2; site numbering of insertions/deletions based on homology with PGK5.

decrease being most pronounced in PGK123. Small-angle neutron diffraction has shown that PGK123 is in an open, extended form with little or no kringle–kringle interaction (Ramakrishnan et al., 1991). Similar studies of native PG show that it exists in a compact, prolate ellipsoidal form that undergoes a large ligand-induced conformational change upon binding at a lysine binding site other than PGK1 (Mangel et al., 1990). The secondary structure remains intact through the conformational change so that the closed conformation results from kringle–kringle and/or kringle–catalytic domain interactions. The lysine binding, therefore, disrupts the domain–domain associations, but because PGK123 binds fibrin, both the closed and open conformations are capable of lysine binding.

Three-dimensional structures have been determined of a number of kringles by crystallography: PTK1 (Tulinsky et al., 1988b; Seshadri et al., 1991), PTK2 (Arni et al., 1993), PGK1 (Wu et al., 1994), PGK4 (Mulichak et al., 1991), and t-PAK2 (de Vos et al., 1992). Additionally, the crystal structure of PGK4 complexed with ACA (Wu et al., 1991) and the NMR structure of ACA-t-PAK2 (Byeon & Llinas, 1991) have been reported. However, no multiple kringle structures have yet been determined, although the Gla-domain–kringle interaction is described in the structure of Ca-PTF1 (Soriano-Garcia et al., 1992) and a kringle–catalytic domain association was revealed with the structure determination of the noncovalent PTK2–PPACK–thrombin complex (Arni et al., 1993). The only apparent common underlying principles surfacing from a cursory examination of the crystal packing interactions of the different kringle crystal structures are the propensity of the lysine binding site to interact with lysine or arginine residues of neighboring molecules and the solvation of the site by an inorganic anion or two.

We describe here crystal structures with (1) 2 kringle (monoclinic crystals of PGK4) and (2) 3 kringle molecules (t-PAK2) per asymmetric unit, which have noncrystallographic kringle–kringle interactions that may approximate such associations in multiple kringle domain molecules. An X-PLOR refined structure of t-PAK2 and the orthorhombic crystal form of PGK4 (1 molecule per asymmetric unit) have been reported previously. The t-PAK2 structure has been refined further here using restrained least-squares methods with noncrystallographic symmetry restraints implemented in the program PROFFT (Finzel, 1987) to produce a more precise geometrical structure and a more realistic assignment of thermal parameters; the monoclinic PGK4 structure has been determined de novo and refined similarly. The t-PAK2 structure has an open-ended 3-fold helical-like arrangement in crystals, whereas monoclinic PGK4 has 2 different 2-fold helical-like arrangements because of additional intermolecular contacts. The interkringle interactions in t-PAK2 are ligand-like, involving lysine residues and lysine binding sites between the independent molecules in the asymmetric unit, whereas those of PGK4 are more extensive and intricate van der Waals contacts, with some hydrogen bonding that does not involve the lysine binding site. All 3 interactions could be operative in multikringle domain molecules.

Results

PGK4

The structures of the 2 PGK4 molecules in the asymmetric unit extend from Cys 1 to Cys 80 (Fig. 1A; see Kinemage 1). No electron density was observed for the interkringle regions of both molecules, similar to and for similar reasons to PGK4 in the orthorhombic crystals (Mulichak et al., 1991) and the ACA–PGK4 complex (Wu et al., 1991). The electron density of the Cys 1–Cys 80 disulfide link was not as good as that of the other 2 disulfides, most likely the result of the flexibility of the interkringle regions. The *cis* peptide bond observed at Pro 30 of other kringle structures (Mulichak et al., 1991; Seshadri et al., 1991; Wu et al., 1991) was not found in either molecule of monoclinic PGK4. The electron density in this region, however, is not well defined in one of the molecules. The individual molecules in the

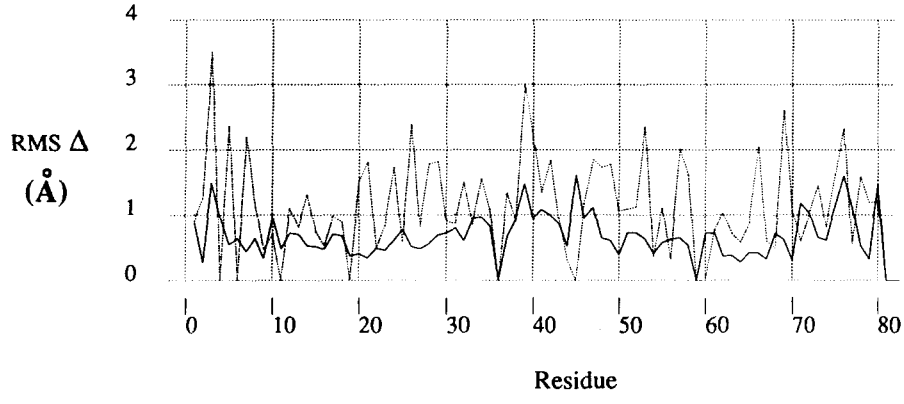

Fig. 2. RMS deviation between the independent molecules of PGK4. Backbone deviations are solid lines; side-chain deviations are dotted lines.

asymmetric unit have a similar folding (Fig. 2). The RMS deviation between the Cα atoms of the 2 molecules is 0.71 Å (0.47 Å omitting 26 differences >0.7 Å); however, there are significant differences between side-chain atoms, which have an RMS deviation of 1.4 Å (Fig. 2). The overall folding of both the molecules is very similar to that of PGK1 (Wu et al., 1994), orthorhombic PGK4 (Mulichak et al., 1991), ACA-PGK4 (Wu et al., 1991), and PTK1 (Seshadri et al., 1991), but is different from t-PAK2 (de Vos et al., 1992), PTK2 (Arni et al., 1993), and the kringle of UK (Li et al., 1992). The RMS deviation between Cα atoms of the orthorhombic and monoclinic PGK4 structures is 0.44 Å and is 1.3 Å on side-chain atoms, which corresponds closely to the differences between the 2 molecules in the asymmetric unit.

An examination of the packing arrangement of PGK4 reveals that each independent molecule makes some close contacts with 5 other molecules, 3 of them extensively, giving rise to a 3-dimensional network. The large number of interkringle contacts is directly related to the high protein fraction of 66% of PGK4. Although some of the contact regions are so minimal as to be insignificant, the interactions of other regions may be relevant to kringle-kringle interactions in multikringle structures such as PG, apolipoprotein [a], and possibly hepatocyte growth factor. A total of 5 different noncrystallographic symmetry interactions occur between the independent molecules (designated A and B hereafter) in the monoclinic crystal form. The resulting units will be referred to as dimers.

Dimer 1 (AB)

The A and B molecules in this interaction are those of the chosen asymmetric unit and are related by a noncrystallographic 2-fold rotation axis approximately parallel to the crystal a^*-axis. From Figure 3 and Kinemage 1, it can be seen that the AB dimer has few noncrystallographic 2-fold interactions between molecules (Arg 10(A) O–Gly 11(B) CA, 3.2 Å; Thr 12(A) OG1–Arg 10(B) O, 3.3 Å; Met 48(A) CE–Met 48(B) CE, 3.3 Å). These are van der Waals contacts of the outer kringle loops (Fig. 1A) and appear to be crystal contacts between dimers rather than those of a dimer molecule.

Dimer 2 (A'B)

This local 2-fold dimer interaction arises from the unit translation of molecule A of the AB dimer along the crystallographic *b*-axis to molecule A' (Fig. 3). As in the case of the AB dimer, there are only 3 van der Waals contacts between the molecules (Pro 68(A') O, Ser 69(A') CA, Ser 69(A') O with Gln 34(B) NE2: 3.5, 3.4, 3.3 Å, respectively) so the association again appears to be only a dimer-dimer contact.

Dimer 3 (AB')

The AB' dimer is generated by applying the crystallographic 2_1 screw axis symmetry to molecule B. Molecule B' generated in this manner is related to A by an approximate rotation of 180° and a translation of about 21 Å along the c^* direction (Fig. 4). The translation is about 2.0 Å less than half of the unit cell length of the *c*-axis and makes the noncrystallographic symmetry relating A and B' an approximate 2_1 screw axis along the c^* direction. However, because the intermolecular contacts between B' and A of the next unit cell are few (Fig. 5), the noncrystallographic symmetry leads to a dimer approximation rather than an infinite 2-fold helical column. Thus, the arrangement of the molecules of monoclinic PGK4 crystals has pseudo $P22_12_1$ sym-

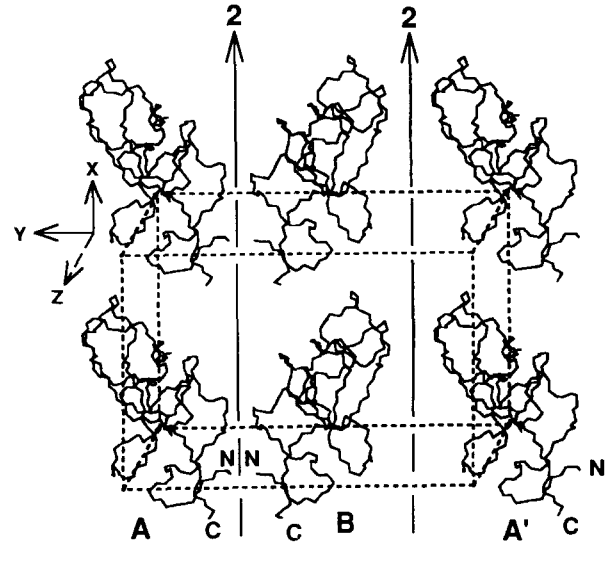

Fig. 3. Two-dimensional network of local 2-fold dimers AB and A'B of PGK4. Local 2-fold axes indicated appropriately; viewed approximately along the *c*-axis.

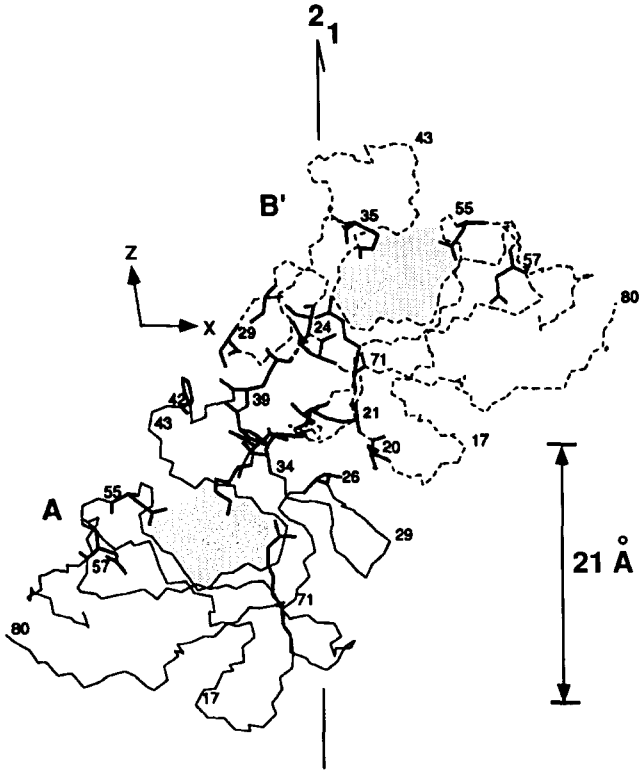

Fig. 4. AB′ dimer of PGK4. Backbone shown thin or broken; side chains in dimer interface and lysine binding site shown in heavy lines; hydrogen bonds, heavy broken lines; lysine binding site, speckled; noncrystallographic 2_1 screw axis shown appropriately.

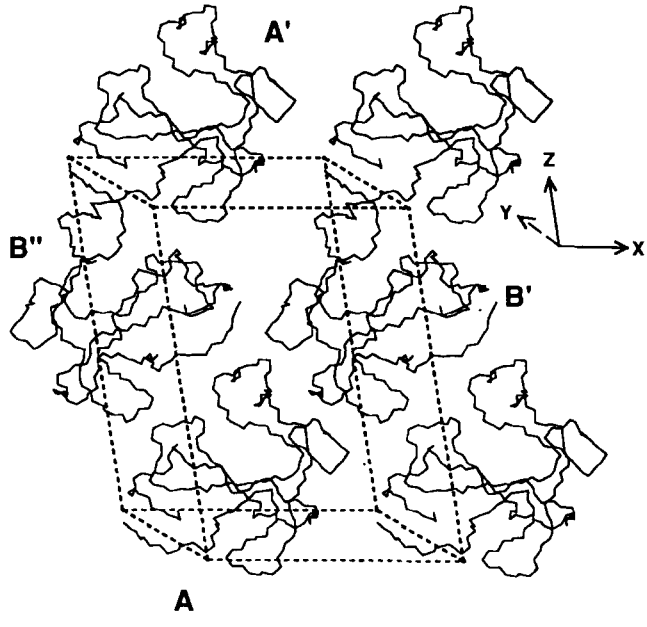

Fig. 5. Two-dimensional network of the AB′, AB″, and A′B″ dimers of PGK4. Backbones only; viewed along crystallographic *b*-axis; same orientation as in Figure 4.

metry. In fact, the intensities of the (00*l*) reflections with $l = 2n + 1$ are generally weak compared to $l = 2n$, as to be expected from such a packing arrangement. From Figure 4, it can be seen that the kringle-kringle contact interface of the AB′ dimer is both extensive and intimate. There are a total of 16 contacts less than 3.5 Å between A and B′ (2 hydrogen bonds and 12 heteronuclear and 4 homonuclear van der Waals contacts) (Table 1). The second outer loop of one molecule of the dimer makes contacts with small segments of the outer loops and the second inner loop of the other molecule. The interkringle interface interactions are generally dipolar, and those of 1 molecule are concentrated between Thr 37 and Glu 39 (12 of 16 contacts), where residues Thr 37, Glu 39, and Thr 66 are particularly involved (Table 1). All of this is accomplished without blocking the lysine binding sites in the AB′ dimer (His 31–Lys 35, Pro 54–Lys 58, Pro 61–Phe 64, Arg 71–Cys 75) (Fig. 4) (Tulinsky et al., 1988a; Mulichak et al., 1991; Wu et al., 1991). It is notable that the ACA-PGK4 complex (Wu et al., 1991) has the same intermolecular interface as AB′ dimers, but between molecules related by a crystallographic 2_1 screw axis.

Dimer 4 (AB″)

Unit translation of the B′ molecule along the *a*-axis gives another dimer interface with molecule A, producing the AB″ dimer (Fig. 5); the molecules in this dimer are also related by an approximate 2_1 screw axis along the c^* direction (Fig. 6). Unit translation of A along the c^* direction produces a similar dimer interface (A′B″): AB″ and A′B″ are related by a unit translation, but the noncrystallographic 2_1 screw axis symmetry makes the kringle-kringle contacts slightly different so that the A′B″ dimer is very similar to AB″ (Fig. 5). Thus, this noncrystallographic element continues the AB″ interaction and leads to an infinite helical column. Molecule A makes 13 contacts <3.5 Å with B″ (Table 2), and the residues involved are different from those of the AB′ dimer. The interactions are marginally more dipolar in the AB″ interface (1 hydrogen bond and 10 heteronuclear and 3 homonuclear van der Waals contacts). The inter-

Table 1. *Intermolecular contacts <3.5 Å involving the AB′ dimer of PGK4*

Molecule A		Molecule B′		Distance (Å)	Interaction
Ser 26	OG	Lys 20	CD	3.3	
Ser 26	OG	Lys 20	CE	3.4	
Gln 34	OE1	Lys 21	NZ	3.0	H bond
Thr 37	CG2	Thr 66	OG1	3.1	
Pro 38	O	Thr 29	OG1	3.3	
Pro 38	CG	Thr 66	O	2.9	
Glu 39	OE1	Gln 23	CA	3.2	
Glu 39	OE1	Gln 23	C	3.4	
Glu 39	CD	Ser 24	N	3.3	
Glu 39	OE1	Ser 24	N	2.8	H bond
Glu 39	OE2	Ser 27	CB	3.5	
Glu 39	OE2	Ser 27	OG	3.5	
Glu 39	O	Thr 29	CG2	3.4	
Glu 39	CB	Thr 66	CG2	3.0	
Glu 39	CG	Thr 66	CG2	3.3	
Pro 42	CB	Thr 29	OG1	3.4	

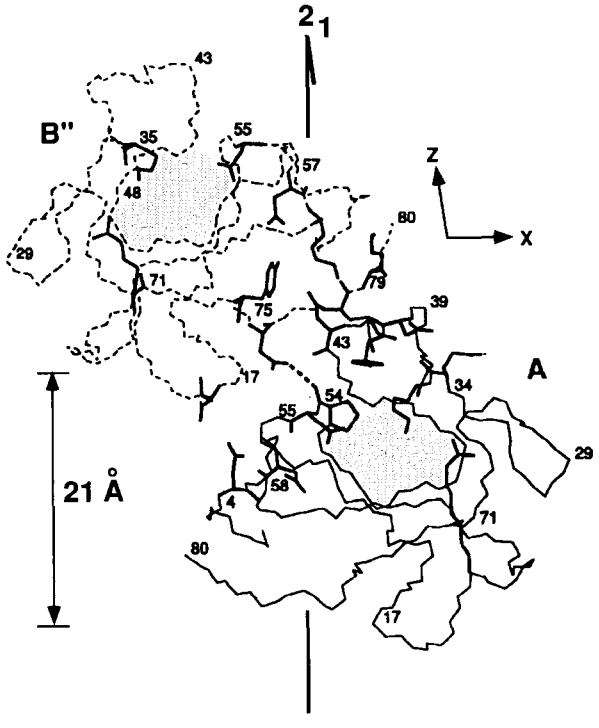

Fig. 6. The AB″ dimer of PGK4. Backbone shown thin or broken; side chains in dimer interface and lysine binding site shown in heavy lines; hydrogen bond, heavy broken line; lysine binding site, speckled; non-crystallographic 2_1 screw axis shown appropriately.

actions essentially involve the second outer loop of one molecule and the second inner loop of the other molecule. Residues Asn 40–Asn 43 of A and Lys 78 of B are heavily involved in the association. Again, the lysine binding sites are not blocked in this dimer.

Table 2. *Intermolecular contacts <3.5 Å involving the AB″ dimer of PGK4*

Molecule A		Molecule B″		Distance (Å)	Interaction
Asp 5	OD1	Thr 18	O	3.5	
Gln 34	O	Lys 78	NZ	3.5	
Asn 40	OD1	Lys 78	CD	3.2	
Asn 40	OD1	Lys 78	NZ	3.5	
Asn 40	O	Lys 79	N	3.2	
Tyr 41	CE2	Lys 78	CD	3.1	
Tyr 41	CZ	Lys 78	CD	3.2	
Tyr 41	OH	Lys 78	CD	3.1	
Tyr 41	OH	Lys 78	CE	3.4	
Asn 43	OD1	Lys 58	NZ	3.4	
Asn 43	ND2	Tyr 74	CG	3.4	
Asn 43	ND2	Tyr 74	CD2	3.4	
Pro 54	O	Asn 76	ND2	3.1	H bond

t-PAK2

All 3 molecules of t-PAK2 in the asymmetric unit are well defined in electron density and extend from Ser-b to Ser 81 (Fig. 1B; see Kinemage 2). Three chloride ions are also present in the structure, 1 in each molecule. The presence of chloride ions agrees with the observation that even relatively low concentrations of chloride ion can precipitate the protein and, in the absence of chloride ion, crystals do not grow (de Vos et al., 1992). The chloride ions, which are in the interface between molecules, are fully occupied and have relatively small thermal parameters (~16 Å^2) compared to the kringle molecules ($\langle B \rangle$ about 22 Å^2). The ions make interactions with the main-chain amide atoms of Val 34, Tyr 35, and His 64 NE2 (Fig. 7), with Cl-N distances of 3.2, 3.2, and 4.0 Å, respectively; the latter appears to be an ion-pair interaction with the imidazolium ion of His 64. Water 339 bridges His 64 ND1 and Thr 71 O through hydrogen bonds, and the

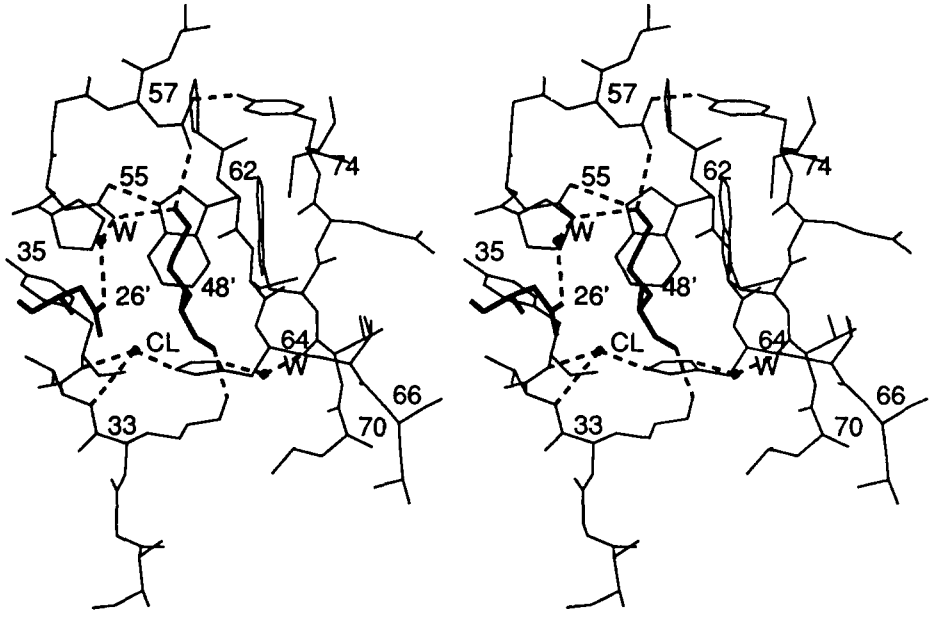

Fig. 7. Intermolecular ligand-like binding interaction in lysine binding site between independent t-PAK2 molecules. Lys 48′ and Asn 26′ of neighboring molecule of trimer shown in bold; chloride ion and water molecule designated; hydrogen bonds and chloride interactions, broken lines.

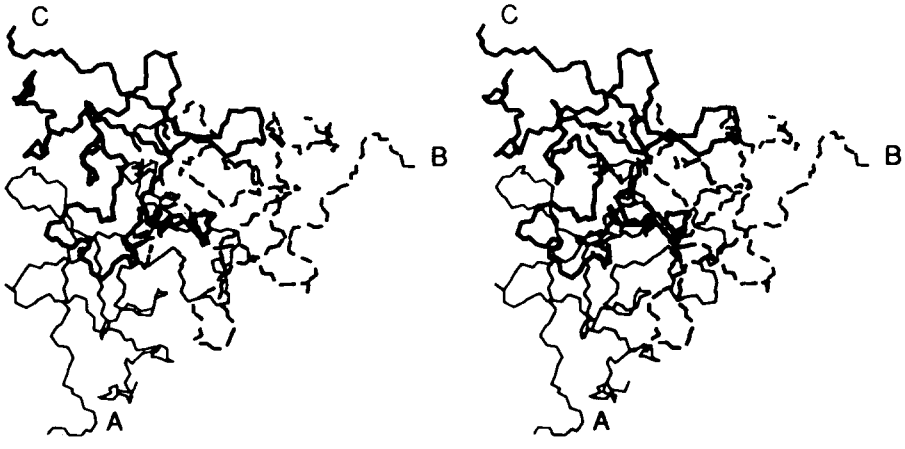

Fig. 8. Stereo view of 3 t-PAK2 molecules of asymmetric unit. Molecule A shown with thin lines, B with broken lines, and C with thick lines; viewed along *a*-axis and noncrystallographic 3_1 screw axis.

chloride is 3.3 Å from Asn 26 ND2 of a neighboring molecule. Another important hydrogen bonded solvent bridge occurs between water 386 and Asn 26 ND2 and Asp 55 OD2 of different molecules (Fig. 7).

The 3 molecules in the asymmetric unit of t-PAK2 are related to each other by a noncrystallographic 3_1 screw axis nearly parallel to the crystal *a*-axis (Figs. 8, 9; Kinemage 2). Because the contacts between noncrystallographic trimers continue and are observed between molecules A and B′, the latter related to B by a unit translation along the *a*-axis (Fig. 9; Table 3), the t-PAK2 molecules are arranged in an infinite helical column. Not surprisingly, then, the continuing interaction along the noncrystallographic 3_1 screw axis enhances crystal growth along the *a* direction (de Vos et al., 1992). Other intermolecular contacts between t-PAK2 molecules are relatively minor, in agreement with the smaller 46% protein fraction of crystals. The most significant kringle–kringle interaction occurs between the lysine binding site of one molecule and the side chain of Lys 48 of a neighboring molecule, where Lys 48 makes 8–9 close contacts (Fig. 7; Table 3). The lysine binding residues are Asp 55 and Asp 57, which form the anionic component of the lysine binding site in t-PAK2, the same as in PGK1 and PGK4. The Trp 62 and Trp 72 residues have close van der Waals contacts with the methylene groups of the lysine ligand (Table 3). The cationic center is Lys 33, capable of interacting with the negatively charged carboxylate of lysine or lysine analogs (de Vos et al., 1992), in agreement with the binding observations of ACA and related compounds with strategically modified site-directed mutants of t-PAK2 (De Serrano et al., 1992). The NZ of Lys 48 from a neighboring molecule forms hydrogen bonded ion pairs with Asp 55 OD2 and Asp 57 OD2 (Figs. 7, 9; Table 3), and the carbonyl oxygen of Lys 48 is hydrogen bonded with Lys 33 NZ. The binding association between t-PAK2 molecules mimics a t-PAK2–fibrin binding mode and resembles that found in the

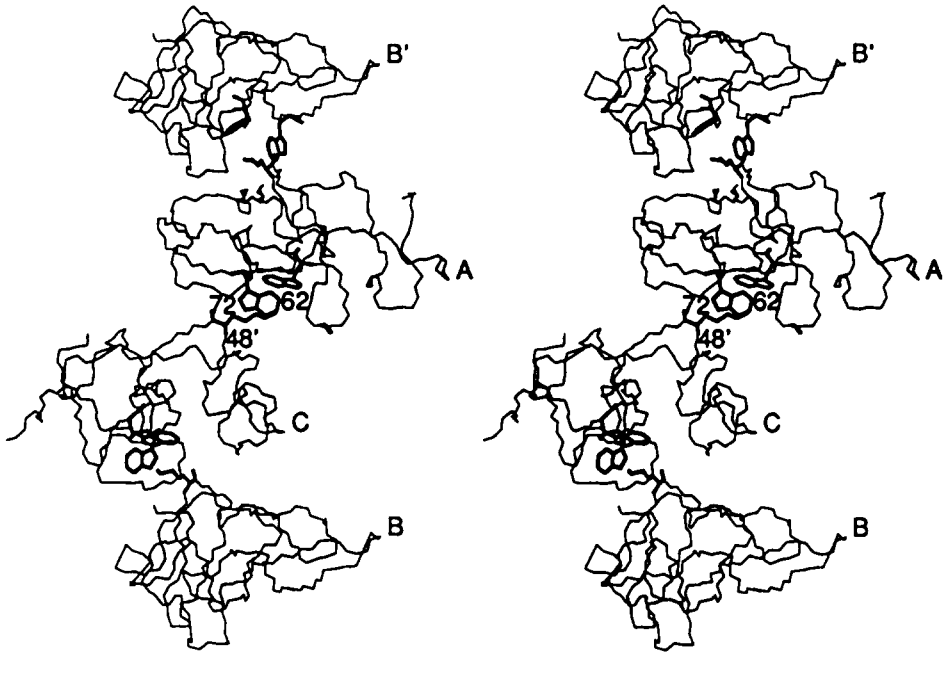

Fig. 9. Stereo view of repeating unit of the infinite 3_1 screw helical chain of t-PAK2 molecules. Lysine binding site identified with Trp 62 and Trp 72.

Table 3. *Intermolecular contacts <3.5 Å in the lysine binding site of t-PAK2*

Molecule 1		Molecule 1′		Distance (Å) A–B*[a]	C–A	B–C	Interaction
Pro 24	CG	Val 34	CG2	3.3	3.4		
Asn 26	OD1	Val 34	CG2			3.4	
Asn 26	ND2	Tyr 35	CE2	3.4			
Asn 26	ND2	WAT[b]		2.9	2.5	2.9	
WAT		Asp 55	OD2	2.6	2.5	2.6	
Met 28	SD	Tyr 35	OH	3.2			
Met 28	CE	Asn 41	ND2			3.1	
Lys 48	O	Lys 33	CE	3.0	3.4		
Lys 48	O	Lys 33	NZ	3.5	2.9	2.6	H bond
Lys 48	NZ	Asp 55	OD2	2.8	3.1	2.8	H bond/ion pair
Lys 48	CE	Asp 57	OD2	3.4	3.5		
Lys 48	NZ	Asp 57	CG	3.5			
Lys 48	NZ	Asp 57	OD2	2.4	2.6	2.8	H bond/ion pair
Lys 48	NZ	Trp 62	CE2			3.5	
Lys 48	CE	Trp 72	CE2	3.2	3.4	3.3	
Lys 48	CE	Trp 72	CZ2	3.2	3.4	3.4	

[a] B* is related to B of B–C by a unit translation along the *a*-axis (Fig. 9).
[b] WAT = Wat 337, Wat 623, and Wat 386 for AB*, CA, and BC interactions, respectively.

ACA–PGK4 complex (Wu et al., 1991). Unlike the AB′ dimer of PGK4, the t-PAK2 crystal structure does not produce any separately identifiable trimer units.

The 3 molecules in the asymmetric unit of t-PAK2 have practically the same folding (RMS deviation ~0.35 Å) (Table 4). Most of the side chains even have similar conformations between the molecules (notable exceptions are His 13, Met 28, and Arg 68). The deviation of His 13 is due to ND2 making a hydrogen bond with Tyr 9 OH at a distance of 2.8 Å in molecules A and C but not in B. This observation is consistent with NMR NOE observations and acid/base titration experiments (Byeon et al., 1989), which found 2 side-chain positions for His 13, one located on the kringle surface (as in molecule B) and the other making intramolecular interactions with other residues (as in molecules A and C). The Met 28 residue is located on the kringle surface, is exposed to solvent, and shows different conformations in all 3 molecules. This is the source of the large deviation of sulfur atoms in Table 4. Residue Arg 68 has different side-chain conformations in molecules A and B. In molecule B, it makes intermolecular contacts along the crystallographic 2_1 screw axis with the N-terminal of molecule C, while in molecules A and C, the side chain is exposed to solvent; little or no electron density describes the side chains of Asn 67–Arg 69 in molecule C. Although t-PAK2 has 5 and 4 more residues than PGK1 and PGK4 respectively, its folding conformation is generally similar to these kringles but for a major exception consisting of 2 turns of distorted α-helix in the Thr 37–Leu 44c segment. The region corresponds to a 3-residue insertion (Fig. 1B) and Pro 42 that distorts the helix. A twist of the β-strand between His 64 and Leu 70 of the second inner loop also occurs with respect to the PG kringles. In the PTK2–thrombin complex, this same region appears to be flexible conformationally and undergoes a hinge movement upon complex formation (Arni et al., 1993).

Table 4. *RMS deviations among the 3 molecules of t-PAK2 in the asymmetric unit*[a]

	A–B	A–C	B–C
All protein atoms	0.83	0.49	0.68
Main chain	0.34	0.30	0.40
Carbonyl oxygens	0.45	0.42	0.53
Side chains	1.16	0.63	0.88
Sulfurs (Cys, Met)	0.82	0.70	1.43
Sulfurs (without Met 28)	(0.54)	(0.32)	(0.70)
Carbon alpha	0.35	0.31	0.41

[a] Molecules of the asymmetric unit are designated A, B, and C. RMS deviations are in Ångstroms.

Discussion

The most notable aspects of the monoclinic form of PGK4 are the 2 independent molecules in the asymmetric unit and the noncrystallographic symmetry elements that associate them in the crystal structure (Kinemage 1). The 2 molecules can be formally thought of as associating into dimer molecules. This approximation will depend to some extent on the intimacy and the extent of the contact between molecules. There are 2 different kinds of noncrystallographic symmetry elements in PGK4: (1) a 2-fold rotation axis approximately parallel to the a^* direction, producing AB and A′B-type dimers, and (2) an approximate 2-fold rotation coupled with a 21-Å translation along the c^* direction, producing dimers AB′ and AB″. Because the translation

is only about 2 Å less than the c^* translation, the latter dimers result from a noncrystallographic 2-fold screw-like operation, which leads to helical-like columns similar to t-PAK2 in the case of AB″ (Fig. 5). The B′ molecule of AB′ is related to B by a strict crystallographic 2_1 screw axis operation while B′ and B″ are separated by a unit translation along the *a*-axis. Because the noncrystallographic 2_1 screw axis contacts between AB′ dimers are few (Fig. 5), a separate dimer results.

The AB and A′B dimers only have 3 intermolecular contacts <3.5 Å each between independent molecules. These are van der Waals interactions involving the outer kringle loops in AB, while in A′B, only Gln 34 of one molecule interacts with the second inner loop of the other. The contacts are so few as to make these dimer-like associations insignificant.

The AB′ and AB″ dimers, however, have many more interface contacts, some of which are hydrogen bonds (Tables 1, 2). Moreover, the AB′- and AB″-type noncrystallographic kringle–kringle interactions do not make use of nor interfere with the lysine binding sites of either molecule (Figs. 4, 6). Thus, the binding site in these associations is exposed and is capable of binding ligands such as lysine of fibrin. The screw axis symmetry element displayed by these dimers lends itself to multikringle structures. Symmetry operations without a translational component, such as the 2-fold rotation of the AB-type dimer, are a closed element and relate only a finite number of objects, whereas the screw axis symmetry of the AB″-type dimer and that of t-PAK2 is unbounded and is capable of relating a large number of objects. The latter could be applicable to the 2 kringles of PT (if terminated as in the AB′ dimer) and is equally compatible with some of the consecutive kringles of PG or the 37 copies of PGK4 in apolipoprotein [a]. The linear distance between the N- and C-terminals of the adjacent kringles in AB′, AB″ dimers, and t-PA trimers is about 53, 33, and 45 Å, respectively, so only longer interkringle peptide segments can satisfy these particular arrangements. For the interkringle peptide to circumnavigate such dimers or multimers, their lengths would have to be at least twice the linear distances. This eliminates certain kringle–kringle interactions from possibly having the translational components observed here (K1–K2 of TPA, K1–K2 and K3–K4 of hepatocyte growth factor, and K1–K2 and K2–K3 of PG, which only have 6, 4, 7, 3, and 12 peptide interkringle segments, respectively). The remaining interkringle peptides are sufficiently long (16–36 residues) to satisfy the screw axis symmetry. It is of note that the interkringle peptides of apolipoprotein [a] are 36 units long, and one is 28 units long. The foregoing considers essentially extended structures for interkringle segments; the situation changes if such regions have secondary or other folded structures. Thus, although kringles may be related by closed elements or combinations thereof in some multikringle molecules, partial unbounded elements are a viable possibility. Presently, there is no evidence to the contrary of such screw-like associations in multikringle structures that are supported by the crystal structures described here.

The surface of the kringle subunits that is buried in the interfaces between them in the oligomeric structures is about the same for the AB′ and AB″ 2_1 screw dimers (1,600–1,700 Å^2) and the 3_1 screw trimers of t-PAK2 (1,791 Å^2). This corresponds to approximately 40% of the monomer surface and compares favorably with comparably sized monomeric and oligomeric proteins (Miller et al., 1987). In addition, the intermolecular contact between molecules of ACA–PGK4 (Wu et al., 1991), which mimics the AB′ dimer interface, buries 1,854 Å^2. Because this contact is an important one for the crystal structure, the interfaces of the AB′ and AB″ dimers and the trimers of t-PAK2 (see Kinemage 2) must likewise produce an energetically stabilizing effect. The AB′ dimer interface may be of more general utility because it is also found in the intermolecular contact between 2_1 screw axis-related molecules in ACA–PGK4 (Wu et al., 1991). Examination of Tables 1 and 2 and intermolecular crystal contacts in ACA–PGK4 and other kringle structures indicates that the 20–27 and 37–45 regions or parts thereof are involved in interkringle contacts to greater or lesser extents. These "sticky" surface regions are at the beginning and toward the end of the second outer loop (Fig. 1). However, the complementary kringle segments with which they interact are not as well defined, although the end of the second inner loop seems to be favored, particularly the tetrapeptide stretch between the last 2 disulfide residues. The 20–27 and 37–45 segments correspond to regions with little sequence homology in different kringles (Tulinsky et al., 1988b). Such diversity could be a factor in producing varied kringle–kringle interfaces. Additional diversity could result from the different folding conformations that these same regions display, as in t-PAK2, PTK2, and the UK kringle.

Another aspect of the AB′ and AB″ dimers is that the kringle–kringle interface does not block the lysine binding site (Figs. 4, 6). This is an essential requirement for the recognition functions of PG and t-PA through certain of their kringle modules that bind fibrin in the activation of PG to plasmin. Thus, access of the lysine binding site of these particular kringles of multikringle molecules is an ultimate necessity. The binding site of PGK4 is not available to chemical modifiers in native PG, and the lysine affinity is expressed by K1 of PGK123 (Vali & Patthy, 1982). Native PG exists in a compact ellipsoidal form that undergoes a large ligand-induced conformational change upon binding lysine (Mangel et al., 1990), which is widely thought to involve the disruption of an interaction between the N-terminal peptide and a kringle. The heavy chain is capable of combining and interacting with ACA, whereas the catalytic domain is not. This indicates plasmin inhibition by ACA is caused by conformational changes in the kringle regions (Rickli & Otavsky, 1975), suggesting kringle–kringle associations must exist in the intact native molecule that are disrupted. These could be the van der Waals–hydrogen bonding type found in the PGK4 dimers, or some may involve lysine binding associations like those of the t-PAK2 trimers for kringles not required in or incapable of fibrin binding. The latter type of interaction has also been observed in the PTK2–PPACK–thrombin complex, where a number of hydrogen bonded salt bridges are formed between arginines of the highly electropositive heparin binding site of thrombin and negatively charged groups of an enlarged anionic center in PTK2 corresponding to the lysine binding site of lysine binding kringles (Arni et al., 1993).

The lysine binding site region of kringles appears to be a source of powerful electrostatic force with a propensity to interact with electropositive centers such as lysine (in t-PAK2) and arginine (in the heparin site of thrombin). Other examples of such charge associations are intermolecular crystal packing interactions in PGK1 (with lysine) and orthorhombic PGK4 (with arginine). However, the polarity of the lysine binding site of kringles can change drastically by selective sequence differences, as in the kringle of UK, where the anionic center reverts to a cationic one by virtue of the Arg 52–Arg 59 sequence

(RNPDNRRR). The difference leads to a polyanion binding affinity for low molecular weight heparins and other negatively charged substances (Stephens et al., 1992). In such cases, new and very different kinds of electrostatic kringle–kringle interactions are possible and must come into play.

Because kringles can also have different folded structures depending upon their sequence, this too can be another source of complementarity between different kringle domains. For instance, t-PAK2 and PTK2 have helical segments in the second outer loop of their kringles, but they are different, while PGK1, PGK4, and PTK1 have none, whereas the UK kringle has both of the helices (Li et al., 1992). In addition, t-PAK2 has a twist of the His 64–Leu 70 reverse turn that is different from the conformation found in PGK1, PGK4, and PTK1. Based on the comparison of the overall structural homology between these kringles, a sequence alignment results that divides kringle domains into 2 groups (de Vos et al., 1992). An additional source of complementarity among kringles is possible from conformational changes accompanying association at domains. In the PTK2 catalytic domain interaction with thrombin (Arni et al., 1993), a hairpin β-turn of the second inner loop of the kringle pivots by 60° as a unit at Val 64 and Asp 70 in order to enhance the electrostatic interaction with thrombin. The same region has different inherent conformations in t-PAK2 and PGK1, PGK4, and PTK1.

The ligand-like binding interaction of t-PAK2 appears to be an important source underlying kringle–kringle associations involving non-lysine binding kringles. The Asp 55 residue of the anionic center is conserved in most kringles (Tulinsky et al., 1988b; Guevara et al., 1993), whereas Asp 57 and the cationic center display variability. Thus, the ligand-like or simply appositely charged interaction with positively charged residues is always a possibility, as in t-PAK2 and the crystal-packing contacts of PGK1 and other orthorhombic PGK4, while the variability of Asp 57 and the cationic center can influence and even change the nature of the specificity (Guevara et al., 1993). Because most kringles are not functionally involved in lysine or similar binding, where the binding site has to be unoccupied and most likely accessible, these kinds of interactions could be widespread among such kringles.

The binding of anions in the cationic region of the lysine binding site of t-PAK2 is also found in other kringle crystal structures. In PGK1, the positive charges are compensated by 2 chloride ions (Wu et al., 1993) and in orthorhombic PGK4, by a sulfate ion (Mulichak et al., 1991). In all 3 cases, the anionic center is neutralized by either a lysine or an arginine side chain. The interactions in PGK1 and orthorhombic PGK4, however, are not ligand-like. In PGK1, Lys 15 from a symmetry-related molecule makes hydrogen bonds with Asp 55 and Asp 57, but enters the lysine binding site at right angles to its surface; in ligand binding, lysine is embedded in the surface (Wu et al., 1991; de Vos et al., 1992). In orthorhombic PGK4, the interactions involve Arg 32 and Arg 71 of neighboring molecules, but they approach the anionic center from a direction opposite to that expected of ligand; the region is complicated even more by the sulfate ion, which additionally hydrogen bonds with Lys 35 of the same kringle and Lys 58 of a symmetry mate. All the foregoing underscores the intense electrostatic nature of the lysine binding site. It would not be surprising if similar kringle–kringle interactions involving localized anions are found in multikringle molecules.

In summary, examination of different kringle crystal structures does not reveal that kringle–kringle interactions are highly systematic; instead, it implicates some regions of kringles to be more "sticky" than others. One is the lysine binding site, which can participate in ligand-like interactions with a side chain(s) of a neighboring molecule. At this point, such interactions have only been identified involving positively charged side groups; however, if different residues make up the binding site, by virtue of a different kringle sequence, the specifics of the association could become very different. A corollary to the ligand-like principle is the electrostatic association of anions with the binding site, which is found in several kringle crystal structures. From the sequence of the site in PTK2, with 2 aspartate and 2 glutamate residues, cation localization in kringles is also a viable alternative and could assist in kringle–kringle interactions by charge compensation or possibly by bridging negative side groups.

A second hallmark of kringle–kringle interactions is that multikringle structures can and are formed by symmetry elements with a translational component. These lead to more densely packed arrangements compared with their closed symmetry counterparts, especially in relating larger numbers of units; smaller closed symmetry elements, however, could likewise have a place in kringle–kringle associations. The interfaces of both of the symmetry types appear to be dominated by van der Waals contacts accompanied with hydrogen bonding. Mutual complementarity thus becomes an important factor in producing and maintaining stability within the domain–domain interfaces. The contacts are, however, relatively disruptable, whereupon more open associations between folded kringle domains are attainable, as in the case of plasminogen (Mangel et al., 1990), possibly for functional reasons.

Experimental

Monoclinic PGK4

Crystals of the monoclinic form of PGK4 were grown using procedures similar to those described previously (Mulichak et al., 1989, 1991), except that 0.8% *n*-butanol was used as the additive but orthorhombic crystals also form. The monoclinic crystals belong to space group $P2_1$ with unit cell dimensions of $a = 32.73$, $b = 49.09$, $c = 46.15$ Å, $\beta = 100.6°$, 4 molecules per unit cell (2 molecules per asymmetric unit), and 66% protein fraction giving $V_m = 1.86$ Å^3/Da (Matthews, 1968). The crystals are twinned along the c^* direction in a manner similar to α-chymotrypsin (Tulinsky et al., 1973).

Three-dimensional X-ray diffraction data were measured at 2.25 Å resolution from 2 crystals employing a Nicolet P3/F 4-circle diffractometer with a graphite monochromator using a wandering stepscan procedure (Wyckoff et al., 1967). The intensity data were corrected for absorption (North et al., 1968) and intensity decay due to X-ray exposure using procedures similar to those described previously (Mulichak et al., 1991). Of 6,943 possible reflections at 2.25 Å resolution, 4,328 (62%) were taken to be observed (39% between 2.5 and 2.25 Å resolution) based on an unobserved intensity cutoff of $2 \times I_{neg}$, where I_{neg} is the average negative intensity for a given 2θ range.

Twinning correction for PGK4 crystals

When a crystal lattice possesses a rotational symmetry other than the symmetry elements of the space group of the crystal, a twin

crystal results (Yeates, 1988). In such cases, the reciprocal lattices of the crystal and twin can overlap. The resulting diffraction intensities are given by linear combinations of the untwinned intensities of the reflections related by the twinning operation. In order to extract the true intensities from the reflections affected by twinning, the extent of twinning and the intensities of the reflections affected by the twinning operation must be known. Several methods have been proposed to deal with this problem (Tulinsky et al., 1973; Fisher & Sweet, 1980; Yeates, 1988).

In the case of monoclinic PGK4 crystals, the overlap of the crystal and the twin is not exact everywhere, so that only a fraction of the diffraction data is adversely affected by twinning and needs to be corrected. The reciprocal lattices of the crystal and twin of PGK4 are shown in Figure 10, with the a^*- and b^*-axes of the crystal and twin practically coincident and only reflections with $l = 0, 4, 7, 8, 11$, and 15 overlapping with those of the twin. From ω-profiles, it was found that 2 reflections with a ϕ separation of greater than 0.4° could be resolved under the instrumental operating conditions of the diffractometer (take-off angle = 3.5°, ω-spread half width = 0.2°, variable top-bottom, left-right collimator slits, etc.).

The twinned reflections were identified from the angular coordinates calculated for the reflections of the crystal and the twin with a ϕ separation of less than 0.4°. Of about 2,800 reflections to 2.8 Å resolution, approximately 700 satisfied this criterion (~25%). Although reflections with $l = 15$ should be twinned (Fig. 10), this proved not to be the case because the crystal and the twin have a small angular separation along the b^* direction, which increases in separation as a function of the distance from the origin of the reciprocal lattice (thus resolving the $l = 15$ layer of reflections). The orientation matrix of the twin was determined prior to intensity data collection of the crystal. Using this matrix, a 6.0-Å-resolution data set of the twin was measured and used to determine the crystal/twin ratio. The squared structure amplitudes of the crystal and twin gave a ratio of 1.55 for about 200 reflections. The 2.8–2.25-Å-resolution data set was collected from a second crystal to minimize intensity decay due to X-ray exposure. Because the twin ratio of this crystal was only 1.15 on intensities, this data set was not corrected for twinning. Of about 700 reflections, 200 were taken as unobserved after "untwinning." Thus, only 18% of the observed reflections to 2.8 Å resolution were corrected for twinning.

t-PAK2

Crystals of t-PAK2 were grown by the vapor diffusion method by using 4 mg/mL protein, 7% saturated ammonium chloride, and 50 mM ammonium bicarbonate at pH 8.0 and were stored in a similar solution but with 50% PEG3400. The crystals also belong to the monoclinic space group $P2_1$ with $a = 54.80$, $b = 63.58$, $c = 46.58$ Å, $\beta = 106.7°$, 6 molecules in the unit cell (3 molecules per asymmetric unit), 46% protein fraction, and $V_m = 2.7$ Å^3/Da. The X-PLOR refinement of the structure (de Vos et al., 1992) used intensities measured at the Midwest Area Detector Facility at Argonne National Laboratory with a Siemens X-1000 Xentronics multiwire area detector employing graphite monochromated CuK_α radiation with a 0.5-mm collimator from a Rigaku RU200 rotating anode generator operating at 50 kV and 100 mA. A total of 1,800 frames at 2 χ settings (0 and 90°) were measured. The raw data set was processed with the XENGEN package of programs (Howard et al., 1987) and consisted of 30,076 observations that produced 11,621 unique reflections (91%, $R_{merge} = 0.070$) and extended to 2.38 Å resolution. The shell from 2.5 to 2.38 Å had 1,101 of 2,105 possible reflections (52%) with an $\langle I/\sigma(I)\rangle$ of 3.7.

Structure determination/refinement

PGK4

A self-rotation function was calculated by Patterson search methods using the program PROTEIN (Steigemann, 1974) to find the noncrystallographic symmetry element relating the molecules. The highest peak gave a correlation of 7.1σ above the mean, and the angles corresponded to a noncrystallographic 2-fold rotation approximately parallel to the a^*-axis. The fully conserved kringle from the orthorhombic crystal form of PGK4 (Mulichak et al., 1991) was used to determine the orientation of the molecules in the asymmetric unit. The 2 highest solutions had peak heights 6.4 and 4.3σ above the mean, and the rotation matrices of the individual molecules were in agreement with the self-rotation matrix.

The translation search was carried out with the program BRUTE (Fujinaga & Read, 1987). It was initially conducted for the individual molecules in the xz plane (correlation coefficients of 0.31 and 0.22, 4.4 and 4.0σ above the mean, respectively).

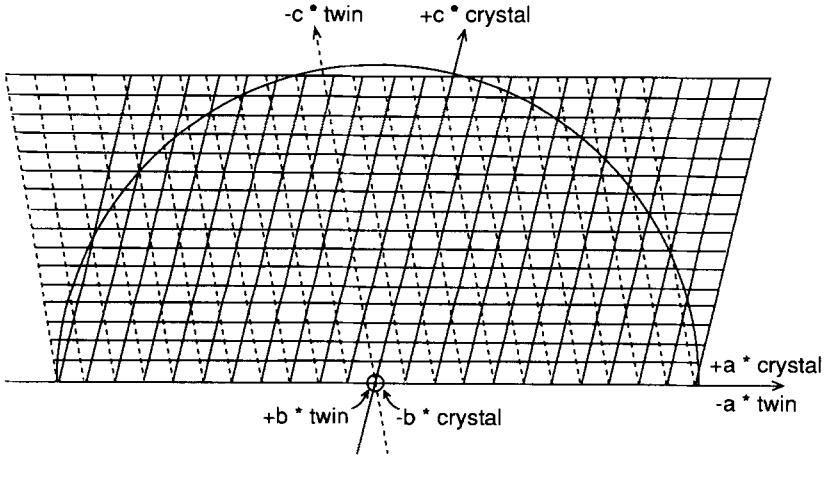

Fig. 10. Reciprocal lattices of the crystal and twin of PGK4. The c^*-axis of the crystal shown by solid line; twin by broken line; layers $l = 0, 4, 7, 8, 11, 15$ of crystal and twin closely overlapped; limiting sphere of 2.8 Å indicated.

Table 5. *Summary of final restrained least-squares parameters/deviations and R-factor statistics of PGK4 and t-PAK2*

	PGK4		t-PAK2	
	Target	RMS deviation	Target	RMS deviation
Distances (Å)				
Bond lengths	0.015	0.015	0.020	0.015
Bond angles	0.030	0.054	0.040	0.046
Planar 1, 4	0.040	0.058	0.060	0.055
Planes (Å)				
Peptides	0.02	0.02	0.02	0.02
Aromatic groups	0.02	0.02	0.02	0.02
Chiral volumes (Å^3)	0.15	0.26	0.15	0.16
Nonbonded contacts (Å)				
Single torsion	0.40	0.24	0.55	0.21
Multiple torsion	0.40	0.35	0.55	0.24
Possible H bond	0.40	0.35	0.55	0.24
Thermal parameters (Å^2)				
Main-chain bond	1.5	1.4	1.5	0.9
Main-chain angle	2.0	1.9	2.0	1.5
Side-chain bond	2.5	2.7	2.0	1.4
Side-chain angle	3.0	3.5	2.5	2.0
Torsion angles (degrees)				
Planar	3.0	3.6	3.0	2.6
Staggered	15	32	15	20
Orthonormal	20	29	20	23
Noncrystallographic symmetry				
Main-chain positional (Å)	0.20	0.38	0.40	0.27
Side-chain positional (Å)	0.40	0.72	0.80	0.44
Main-chain thermal (Å^2)	2.0	1.4	2.0	0.9
Side-chain thermal (Å^2)	3.0	2.2	3.0	1.5

PGK4

Average angle = 117.1 ± 3.6°

Diffraction pattern

$\sigma(|F_o|) = A + B(\sin\theta/\lambda - 1/6)$, where A = 12, B = −60

$\langle||F_o| - |F_c||\rangle = 25$

d_{min}	No. of reflections	$\sigma(\|F_o\|)$	$\langle\|\|F_o\| - \|F_c\|\|\rangle$	*R* value, shell	*R* value, sphere
4.20	560	16.0	37.0	0.159	0.159
3.60	499	14.2	31.2	0.141	0.151
3.20	539	13.1	27.1	0.156	0.152
2.90	574	12.1	22.2	0.166	0.155
2.70	521	11.3	20.5	0.181	0.158
2.50	570	10.5	18.8	0.185	0.161
2.25	722	9.4	17.8	0.194	0.164

t-PAK2

Average angle = 116.8 ± 2.9°

Diffraction pattern

$\sigma(|F_o|) = A + B(\sin\theta/\lambda - 1/6)$, where A = 14.5, B = −120

$\langle||F_o| - |F_c||\rangle = 29$

d_{min}	No. of reflections	$\sigma(\|F_o\|)$	$\langle\|\|F_o\| - \|F_c\|\|\rangle$	*R* value, shell	*R* value, sphere
4.56	1,142	23.3	47.6	0.172	0.172
3.75	1,301	19.8	35.8	0.126	0.147
3.32	1,299	17.4	31.4	0.129	0.142
3.01	1,332	15.5	26.7	0.148	0.143
2.78	1,309	13.7	22.9	0.149	0.144
2.60	1,195	12.1	20.0	0.155	0.145
2.38	1,249	10.6	17.6	0.151	0.145

In order to find the relative position of one with respect to the other along the y-axis, a 3-dimensional search was carried out fixing 1 molecule. This gave an overall correlation of 0.45. A rigid-body refinement produced a correlation of 0.49 and the resulting structure gave a crystallographic R value of 0.45 in the 7.0–2.8-Å resolution range.

The electron density map calculated from these coordinates was subjected to noncrystallographic symmetry averaging. The correlation coefficient was refined during the symmetry averaging. The starting correlation of the electron density was 0.65, and it improved to 0.81 with small adjustments of the position of the noncrystallographic symmetry element.

Using the averaged map, the model was refitted to the electron density by interactive computer graphics with the program FRODO (Jones, 1982). The other molecule was generated by the symmetry operation. The structure was refined employing the restrained least-squares program PROFFT (Finzel, 1987) with noncrystallographic symmetry restrained during refinement. The refinement proceeded in stages, each of which was followed by model building of both molecules in the asymmetric unit using $(2|F_o| - |F_c|)$ and $(|F_o| - |F_c|)$ maps. Using an overall thermal parameter of 20 Å^2, the R value converged at 0.24 in the 7.0–2.8-Å-resolution range. The resolution was extended to 2.5 Å and water molecules were gradually added. In the last stages of refinement, the remainder of the data (to 2.25 Å) were included, and reflection weights were assigned based on the $\langle||F_o| - |F_c||\rangle$ discrepancy in various resolution ranges. The final structure has a crystallographic R value of 0.164 for 3,985 reflections between 7.0 and 2.25 Å resolution with 120 water molecules (occupancies >0.5, about 60 water molecules per PGK4) and an average thermal parameter of 22.5 Å^2. A summary of the final refinement parameters and reflection weights is given in Table 5.

t-PAK2

The starting model for the PROFFT refinement of t-PAK2 was the X-PLOR (Brünger et al., 1987) refined structure (R = 0.184, 3 chloride ions, 92 water molecules) (de Vos et al., 1992). This model, from which the chloride ions and water molecules were removed, gave an R value of 0.26 with an overall thermal parameter of 16 Å^2 using data from 8.0 to 2.8 Å resolution. Refinement of positions overall, then individual thermal parameters, reduced the R to 0.20. Chloride ions were located from a difference electron density map and introduced in the refinement after 32 cycles. As in the case of the PGK4, the noncrystallographic symmetry was restrained with different restraints applied for the main- and side-chain atoms. The remaining diffraction data (to 2.38 Å) were included along with water solvent molecules. The final structure of t-PAK2 has an R value of 0.145 for 8,827 reflections between 8.0 and 2.38 Å resolution with 3 chloride ions, 190 water molecules (about 63 per t-PAK2 with occupancies >0.5), and an average thermal parameter of 21.7 Å^2. A summary of the refinement parameters is given in Table 5. The PROFFT refinement reduced the RMS deviation of bond angles from 3.3° (X-PLOR) to 2.9°, whereas the RMS deviation of the noncrystallographic symmetry was the same for main-chain atoms (0.6 Å) but was smaller for side-chain atoms (1.0–0.88 Å). The largest improvement in the R value came from the addition of more water structure.

Although the extent of diffraction of the PGK4 and t-PAK2 structures is comparable, an examination of the RMS deviations from ideal values (Table 5) suggests better general quality for the t-PAK2 structure. Additionally, underscoring this conclusion is the fact that the restraints imposed on the PGK4 structure were tighter. The twinning of PGK4 crystals is the likely source of the discrepancy. The coordinates of both structures have been deposited in the Brookhaven Protein Data Bank, accession numbers 1PMK (PGK4) and 1PML (t-PAK2), and appear on the Diskette Appendix.

Acknowledgments

We thank Dr. Mary L. Westbrook for making the intensity measurements and processing the data, and Dr. Janet Smith for providing us with the program to perform the symmetry averaging. We thank Drs. A.M. deVos and A.A. Kossiakoff for examining the manuscript and providing helpful comments. This work was supported by NIH grant HL 25942.

References

Arni RK, Padmanabhan K, Padmanabhan KP, Wu TP, Tulinsky A. 1993. Structures of the noncovalent complexes of human and bovine prothrombin fragment 2 with human PPACK-thrombin. *Biochemistry 32*:4727–4737.

Brünger AT, Kuriyan J, Karplus M. 1987. Crystallographic R factor refinement by molecular dynamics. *Science 235*:458–460.

Byeon IL, Kelley RF, Llinas M. 1989. 1H NMR structural characterization of a recombinant kringle 2 domain from human tissue-type plasminogen activator. *Biochemistry 28*:9350–9360.

Byeon IL, Llinas M. 1991. Solution structure of the tissue-type plasminogen activator kringle 2 domain complexed to 6-aminohexanoicacid: An antifibrinolytic drug. *J Mol Biol 222*:1035–1051.

De Serrano VS, Sehl LC, Castellino FJ. 1992. Direct identification of lysine-33 as the principal cationic center of the ω-amino acid binding site of the recombinant kringle 2 domain of tissue-type plasminogen activator. *Arch Biochem Biophys 292*:206–212.

de Vos AM, Ultsch MH, Kelley RF, Padmanabhan K, Tulinsky A, Westbrook ML, Kossiakoff AA. 1992. Crystal structure of the kringle 2 domain of tissue plasminogen activator at 2.4 Å resolution. *Biochemistry 31*:270–279.

Esmon CT, Jackson CM. 1974. Conversion of prothrombin to thrombin. IV. Function of fragment 2 region during activation in the presence of factor V. *J Biol Chem 249*:7791–7797.

Finzel BC. 1987. Incorporation of fast Fourier transforms to speed least-squares refinement of protein structures. *J Appl Crystallogr 20*:53–55.

Fisher RG, Sweet RM. 1980. Treatment of diffraction data from protein crystals twinned by merohedry. *Acta Crystallogr A 36*:755–760.

Fujinaga M, Read RJ. 1987. Experiences with a new translation-function program. *J Appl Crystallogr 20*:517–521.

Gardell SJ, Duong LT, Diehl RE, York JD, Hare TR, Register RB, Jacobs JW, Dixon RAF, Friedman PA. 1989. Isolation, characterization, and cDNA cloning of a vampire bat salivary plasminogen activator. *J Biol Chem 264*:17947–17952.

Gitel SN, Owen WG, Esmon CT, Jackson CM. 1973. A polypeptide region of bovine prothrombin specific for binding to phospholipids. *Proc Natl Acad Sci USA 70*:1344–1348.

Guevara J, Jan AY, Knapp R, Tulinsky A, Morrisett JD. 1993. Comparison of ligand-binding sites of modeled apo[a] kringle-like sequences in human lipoprotein[a]. *Arteriosclerosis Thromb 13*:758–770.

Gunzler WA, Steffens GJ, Otting F, Kim SMA, Frankus E, Flohe L. 1982. The primary structure of high molecular mass urokinase from human urine. The complete amino acid sequence of the A-chain. *Hoppe-Seyler's Z Physiol Chem 363*:1155–1165.

Hochschwender SM, Laursen RA. 1981. The lysine binding sites of human plasminogen: Evidence for a critical tryptophan in the binding site of kringle 4. *J Biol Chem 256*:11172–11176.

Hoover GJ, Menhart N, Martin A, Warder S, Castellino FJ. 1993. The amino acids of the recombinant kringle 1 domain of human plasminogen that stabilize its interaction with ω-amino acids. *Biochemistry 32*:10936–10944.

Howard AJ, Gilliland GL, Finzel BC, Poulos TL, Ohlendorf DH, Salemme FR. 1987. The use of an imaging proportional counter in macromolecular crystallography. *J Appl Crystallogr 20*:383–387.

Jones TA. 1982. FRODO: A graphics fitting program for macromolecules. In: Sayre D, ed. *Computational crystallography*. Oxford, UK: Clarendon Press. pp 303–317.

Li X, Smith RAG, Dobson CM. 1992. Sequential 1H NMR assignments and secondary structure of the kringle domain from urokinase. *Biochemistry 31*:9562-9571.

Magnusson S, Peterson TE, Sottrup-Jensen L, Claeys H. 1975. Complete primary structure of prothrombin: Isolation, structure, and reactivity of ten carboxylated glutamic acid residues and regulation of prothrombin activation by thrombin. In: Reich E, Rifkin DB, Shaw E, eds. *Proteases and biological control*. Cold Spring Harbor, New York: Cold Spring Harbor Laboratories. pp 123-149.

Mangel WF, Lin B, Ramakrishnan V. 1990. Characterization of an extremely large, ligand induced conformational change in plasminogen. *Science 248*:69-73.

Matthews BW. 1968. Solvent content of protein crystals. *J Mol Biol 33*: 491-497.

McLean JW, Tomlinson JE, Wun-Jing K, Eaton DL, Chen EY, Fless GM, Scanu AM, Lawn RM. 1987. cDNA sequence of human apolipoprotein(a) is homologous to plasminogen. *Nature 330*:132-137.

McMullen BA, Fujikawa K. 1985. Amino acid sequence of the heavy chain of human α-factor XIIa (activated Hageman factor). *J Biol Chem 260*:5328-5340.

Miller S, Lesk AM, Janin J, Chothia C. 1987. The accessible surface area and stability of oligomeric proteins. *Nature 328*:834-836.

Mulichak AM, Park CH, Tulinsky A, Petros AM, Llinas M. 1989. Human plasminogen kringle 4: Crystallization and preliminary diffraction data of two different crystal forms. *J Biol Chem 264*:1922-1923.

Mulichak AM, Tulinsky A, Ravichandran KG. 1991. Crystal and molecular structure of human plasminogen kringle 4 refined at 1.9 Å resolution. *Biochemistry 30*:10576-10588.

Myrmel KH, Lundblad RL, Mann KG. 1976. Characteristics of the association between prothrombin fragment 2 and α-thrombin. *Biochemistry 15*:1767-1773.

Nakamura T, Nishizawa T, Hagiya M, Seki T, Shimonishi M, Sugimura A, Tashiro K, Shimizu S. 1989. Molecular cloning and expression of human hepatocyte growth factor. *Nature 342*:440-443.

Nelsestuen GL, Zytkovicz TH, Howard JB. 1974. The mode of action of vitamin K: Identification of γ-carboxyglutamic acid as a component of prothrombin. *J Biol Chem 249*:6347-6350.

Nielsen PR, Einer-Jensen K, Holtet TL, Andersen BD, Poulsen FM, Thogersen HC. 1993. Protein-ligand interactions in the lysine-binding site of plasminogen kringle 4 are different in crystal and solution. *Biochemistry 32*:13019-13025.

North ACT, Philips DC, Mathews FS. 1968. A semi-empirical method of absorption correction. *Acta Crystallogr A 24*:351-359.

Patthy L. 1985. Evolution of the proteases of blood coagulation and fibrinolysis by assembly from modules. *Cell 41*:657-663.

Pennica D, Holmes WE, Kohr WJ, Harkins RN, Vehar GA, Ward CA, Bennett WF, Yelverton E, Seeberg PH, Heynober HL, Goeddel DV, Collen D. 1983. Cloning and expression of human tissue-type plasminogen activator cDNA in *E. coli*. *Nature 301*:214-221.

Ramakrishnan V, Patthy L, Mangel WF. 1991. Conformation of Lys-plasminogen and the kringle 1-3 fragment of plasminogen analyzed by small-angle neutron scattering. *Biochemistry 30*:3963-3969.

Rickli EE, Otavsky WI. 1975. A new method of isolation and some properties of the heavy chain of human plasmin. *Eur J Biochem 59*:441-447.

Seshadri TP, Tulinsky A, Skrzypczak-Jankun E, Park CH. 1991. Structure of bovine prothrombin fragment 1 refined at 2.25 Å resolution. *J Mol Biol 220*:481-494.

Soriano-Garcia M, Padmanabhan K, de Vos AM, Tulinsky A. 1992. The Ca^{2+} ion and membrane binding structure of the Gla domain of Ca-prothrombin fragment 1. *Biochemistry 31*:2554-2556.

Sottrup-Jensen L, Claeys H, Zajdal M, Petersen TE, Magnusson S. 1978. The primary structure of human plasminogen: Isolation of two lysine-binding fragments and one "mini" plasminogen (MW, 38,000) by elastase-catalyzed-specific limited proteolysis. In: Davidson JF, Rowan RM, Samama MM, Desnoyers PC, eds. *Progress in chemical fibrinolysis and thrombolysis, vol 3*. New York: Raven Press. pp 191-209.

Steffens GJ, Gunzler WA, Otting F, Frankus E, Flohe L. 1982. The complete amino acid sequence of low molecular mass urokinase from human urine. *Hoppe-Seyler's Z Physiol Chem 363*:1043-1058.

Steigemann W. 1974. Die Entwicklung und Anwendung von Rechenverfahren und Rechenprogrammen zur Strukturanalyse von Proteinen am Beispiel des Trypsin-Trypsininhibitor Komplexes, des freien Inhibitors und der L-Asparaginase [dissertation]. München: Technische Universitat.

Stenflo J, Fernlund P, Egan W, Roepstorff P. 1974. Vitamin K dependent modification of glutamic acid residues in prothrombin. *Proc Natl Acad Sci USA 71*:2730-2733.

Stephens RW, Bokman AM, Myohanen HT, Reisberg T, Tapiovaara H, Pedersen N, Grondahl-Hansen J, Llinas M, Vaheri A. 1992. Heparin binding to the urokinase kringle domain. *Biochemistry 31*:7572-7579.

Thorsen S, Clemmensen I, Sottrup-Jensen L, Magnusson S. 1981. Adsorption to fibrin of native fragments of known primary structure from human plasminogen. *Biochim Biophys Acta 668*:377-387.

Trexler M, Vali Z, Patthy L. 1982. Structure of the omega-aminocarboxylic acid-binding sites of human plasminogen. Arginine 70 and aspartic acid 56 are essential for binding of ligand by kringle 4. *J Biol Chem 257*:7401-7406.

Tulinsky A, Mani NV, Morimoto CN, Vandlen RL. 1973. The structure of α-chymotrypsin. I. The refinement of the heavy-atom isomorphous derivatives at 2.8 Å resolution. *Acta Crystallogr B 29*:1309-1322.

Tulinsky A, Park CH, Mao B, Llinas M. 1988a. Lysine/fibrin binding sites kringles modelled after the structure of kringle 1 of prothrombin. *Proteins Struct Funct Genet 3*:85-96.

Tulinsky A, Park CH, Skrzypczak-Jankun E. 1988b. Structure of prothrombin fragment 1 refined at 2.8 Å resolution. *J Mol Biol 202*:885-901.

Vali Z, Patthy L. 1982. Location of the intermediate and high affinity ω-aminocarboxylic acid-binding sites in human plasminogen. *J Biol Chem 257*:2104-2110.

Wu TP, Padmanabhan KP, Tulinsky A. 1994. The structure of recombinant plasminogen kringle 1 and the fibrin binding site. *Blood Coag Fibrinolysis*. Forthcoming.

Wu TP, Padmanabhan K, Tulinsky A, Mulichak AM. 1991. The refined structure of the ε-aminocaproic acid complex of human plasminogen kringle 4. *Biochemistry 30*:10589-10594.

Wyckoff HW, Doscher M, Tsernoglou D, Inagami T, Johnson LN, Hardman KD, Allewell NM, Kelley DM, Richards FM. 1967. Design of a diffractometer and flow cell system for X-ray analysis of crystalline proteins with applications to the crystal chemistry of ribonuclease-S. *J Mol Biol 27*:563-578.

Yeates TO. 1988. Simple statistics for intensity data from twinned specimens. *Acta Crystallogr A 44*:142-144.